frontiers in Earth Science

ORIGINAL RESEARCH
published: 25 May 2021
doi: 10.3389/feart.2021.647495

Timing and Mechanisms of the Formation of the Dark Layers in the Sea of Japan During the Last 40 kyr

S. Gorbarenko[1], X. Shi[2], A. Bosin[1], Y. Liu[2], A. Artemova[1], J. Zou[2], E. Yanchenko[1], Y. Vasilenko[1], Y. Wu[2] and L. Hu[2]*

[1]V.I. Il'ichev Pacific Oceanological Institute, Vladivostok, Russia, [2]First Institute of Oceanography, MNR, Qingdao, China

The marginal location of the Sea of Japan and its constrained water exchange with the western Pacific make this sea a subtle subject for the investigation of orbital and suborbital climate changes. However, the response of this unique basin to the climate and sea level changes at the end of the last glaciation and deglaciation and during the Holocene is not fully understood. We provided detailed reconstructions of the dark layers including the timing and mechanisms responsible for their formation, during the last 40°kyr, based on the multiproxy correlation of three cores from the northern and central parts of the sea with well-dated $\delta^{18}O$ records of the Greenland ice and China cave stalagmites. High resolution color photo lightness, the conventional color parameters L* and b*, AMS ^{14}C data, chlorin and carbonate calcium content and pollen climate parameters allowed the correlation of the DLs of these cores with Greenland interstadials (GI), Heinrich stadials (HS) and summer East Asian monsoon intensity. DLs 9, 8, 7, and 6, formed after Heinrich stadials 4 (38.5–39.5°ka), were triggered by GIs 8, 7, 6 and 5, coeval with the intensification of the East Asian summer monsoon and the increase of surface water stratification and productivity. The long-lasting GI 8, accompanied by significant climate warming, led to the formation of the more intense DL 9. The accumulation of DL five was forced by a rapid global sea level fall, coeval with cold HS 3, due to the decrease of saline Tsushima Current water input into the sea, increased surface water stratification and a drop in deep water ventilation. DL four was probably launched by GI 3 and summer East Asian monsoon intensification. Further falls in global sea level during the last glacial maximum led to the formation of DLs 3 and 2 during the periods 27.0–24.2°ka and 23.5–17.0°ka, respectively. DL 1 was associated with significant summer East Asian monsoon intensification and environmental warming at the onset of the Holocene.

Keywords: sea – level change, color proxy, photo lightness, chlorin, pollen indices, climate change, sediment oxygenation

OPEN ACCESS

Edited by:
Steven L. Forman, Baylor University, United States

Reviewed by:
Li Lo, National Taiwan University, Taiwan
Nadia Solovieva, University College London, United Kingdom

****Correspondence:***
S. Gorbarenko
gorbarenko@poi.dvo.ru

Specialty section:
This article was submitted to Quaternary Science, Geomorphology and Paleoenvironment, a section of the journal Frontiers in Earth Science

Received: *30 December 2020*
Accepted: *10 May 2021*
Published: *25 May 2021*

Citation:
Gorbarenko S, Shi X, Bosin A, Liu Y, Artemova A, Zou J, Yanchenko E, Vasilenko Y, Wu Y and Hu L (2021) Timing and Mechanisms of the Formation of the Dark Layers in the Sea of Japan During the Last 40 kyr. Front. Earth Sci. 9:647495. doi: 10.3389/feart.2021.647495

INTRODUCTION

The semi-closed Sea of Japan is connected with the Western Pacific through shallow straits. The strong influence of the East Asian monsoon has caused a very specific paleo-oceanographic history over the Quaternary, which has attracted great attention from the scientific community. For eighty-ninety years of the last century, the results of the oxygen isotope analyses of planktic foraminifera from the Sea of Japan sediments have shown significant lightening its $\delta^{18}O$ values during the last

glacial maximum (LGM) Gorbarenko, (1983); Gorbarenko, (1993); Oba, (1984); Oba et al. (1991); Keigwin and Gorbarenko, (1992); Tada et al. (1995) et so on). Such lightening $\delta^{18}O$ values of planktic foraminifera is contrary to heavy carbonate $\delta^{18}O$ values in the records of the world ocean over the marine isotopic stage (MIS) 2 (Martinson et al., 1987; Lisiecki and Raymo, 2005) and may be explained only by decrease in $\delta^{18}O$ and salinity of the Sea of Japan surface water. Oba et al. (1991) inferred that the decrease in surface water salinity in the Sea of Japan during the LGM can be explained by the influence of the input of freshwater from the Huang He (Yellow) River into the Sea of Japan, through the Tsushima Strait. Alternatively, this could be due to the regional prevailing of precipitation above evaporation and crucial decreased input of the saline Tsushima Current water into the sea *via* the shallow Tsushima Strait (−130 m) forced by remarkable shrinking of water exchange with the Western Pacific during low sea level stand (Gorbarenko, 1983; Gorbarenko, 1993). After an investigation of the ODP Sites, Tada et al. (1995); Tada et al. (1992) concluded that Quaternary sediments in the Sea of Japan are characterized by centimeter to meter scale alternations of dark, organic-rich layers and light, organic-poor layers which occurred synchronously in the basin. Furthermore, they concluded that decimeter to meter scale alternations of dark and light layers were associated with eustatic changes in global sea level, while the centimeter to decimeter scale alternations may be associated with the Dansgaard-Oeschger (DO) cycles, when each dark layer (DL) was deposited during an interstadial (Tada et al., 1992; Tada et al., 1995; Tada et al., 1999). Later, alternations of dark and light layers in the Sea of Japan were investigated further by many researchers and the results reported suggest that different modes of deep water oxygenation at the bottom, connected with deep water circulation and East Asian summer monsoon intensity, were responsible for DLs forming in this unique basin (Kido et al., 2007; Nagashima et al., 2007; Watanabe et al., 2007; Yokoyama et al., 2007; Khim et al., 2009). The sequences of dark and light layers were found in many cores in the Sea of Japan, which were correlated by the color proxy L* and extended back 0.7 My (Tada et al., 1992; Kido et al., 2007; Nagashima et al., 2007). Based on the sites drilled by the IODP Expedition 346, the sequence of the dark and light layers was extended up to 1.45 My (Tada et al., 2018). It should be noted that sequences of dark and light layers, related to Greenland DO cycles, have been observed in other regions (Behl and Kennett, 1996). A color parameter like b*, responsible for the organic content in sediments, was successfully used to correlate the millennial-scale paleo-oceanography events of the East Asian marginal Okhotsk and Bering seas with DO cycles (Nürnberg and Tiedemann, 2004; Riethdorf et al., 2013; Gorbarenko et al., 2019).

Despite the availability of the well-dated millennial-orbital scale paleo-oceanographic investigations of this unique marginal basin (mostly carried out by Japanese and Korean researchers), understanding of the reasons and mechanisms behind the formation of dark and light layers during the last glaciation and deglaciation and during the Holocene remains poor. It is not clearly understood why and when DLs formation related with DO interstadials during glacial time with moderate sea level standing over the last 40°kyr transit into DLs, relating to orbital-scale climate and global sea level changes. There is an uncertainty which reasons and mechanisms forced formation of DLs in the Sea of Japan during this time span and precise ages of DLs.

Here, we studied the formation of dark and light layers, their ages and the reasons behind their origin, during the last 40°kyr, based on three sediment cores recovered from the northern and central parts of the Sea of Japan. We used AMS ^{14}C dating, advanced color and productivity proxies for the correlation of dark and light layers between cores, according to their synchronicity in this basin, and pollen records in order to correlate them with climate change and find their relationship with Greenland Interstadials and Heinrich events. We used the well-dated NGRIP $\delta^{18}O$ record on the GICC05 scale chronology Seierstad et al., (2014) and the record of sea level changes Lambeck et al. (2014), Yokoyama et al. (2018) as a robust framework for the timing of the dark and light layers.

OCEANOGRAPHY AND ATMOSPHERIC SETTING

The Sea of Japan presents a marginal, semi-closed basin connected with the western Pacific and Okhotsk Sea by four shallow passes; the deeper of them, the Tsushima and Tsugaru Straits, have sills with depths of nearly 135 m. The Tsushima Warm Current (TWC), a branch of the Kuroshio Current, enters into the Sea of Japan through the Tsushima Strait, moving northeastward and flowing out into the Pacific through the Tsugaru Strait and partially into the Okhotsk Sea, through the Soya Strait.

The Polar front (located at nearly 40°N) divides the Sea of Japan into two, separated surface water masses. The northern cores (LV32-33 and LV76-3-1) were located under the influence of the cold Liman Current and the central core (LV53-23-1) was located under the influence of the north branch of the TWC (**Figure 1**).

The deep water of the Sea of Japan (to a water depth of ~2000 m) is highly homogenous, with very low temperatures and phosphorous content and high dissolved oxygen due to very active deep water formation and extensive oxygenation (Kim et al., 2002; Talley et al., 2006; Gamo et al., 2014). However, the situation may have been very different in the past, when the density of the surface water decreased due to freshening during drops in global sea level and the cessation (or significant decrease) of the TWC water input in the sea (Gorbarenko, 1983; Gallagher et al., 2015).

On the other hand, the environment, ventilation and sedimentation of the Sea of Japan is strongly influenced by the summer and winter East Asian monsoon, associated with DO cycles at a sub-orbital time scale (Tada et al., 1992; Tada et al., 1999; Nagashima et al., 2007; Nagashima et al., 2011). Therefore, the Sea of Japan presents a unique and subtle basin for the investigation of the climate and environment changes of the Northern Hemisphere over a wide range of time scales.

MATERIALS AND METHODS

We used multiproxy records from three sediment cores, recovered in the Sea of Japan during joint Russian-Chinese

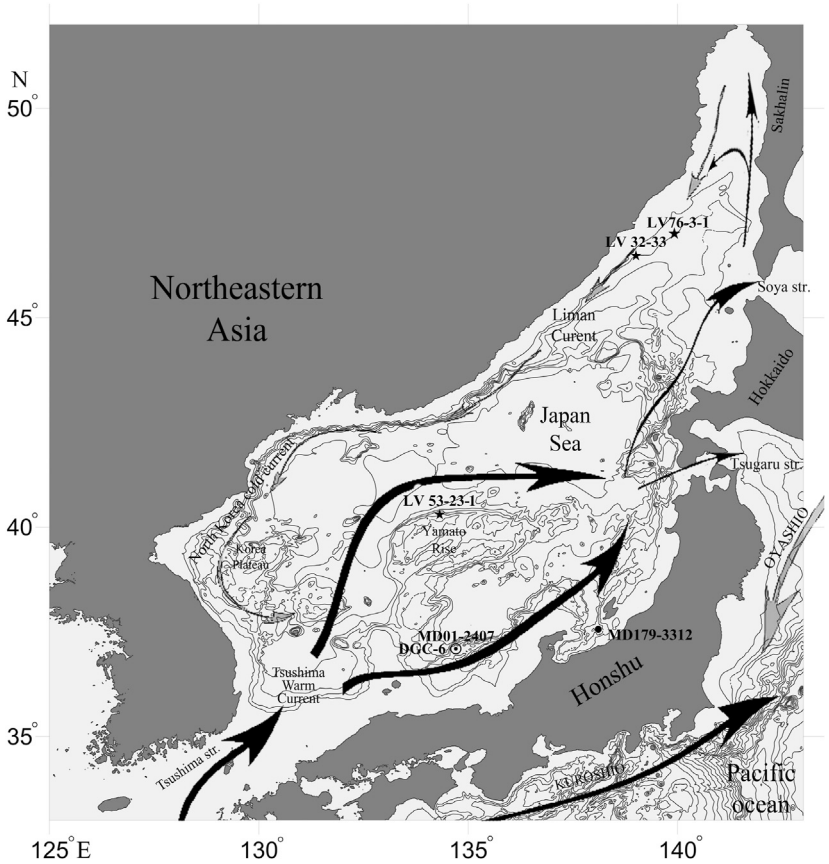

FIGURE 1 | The bathymetric map of the Sea of Japan showing the main surface water currents and the locations of sediment cores LV76-3-1 (studied in present paper), LV32-33 Gorbarenko et al. (2014), LV53-23-1 Gorbarenko et al. (2015), MD179-3312 Ishihama et al. (2014) and MD01-2407 and DGC-6 Yokoyama et al. (2007).

expeditions (**Figure 1**). The northern core (LV76-3-1), recovered from the base of the Primorye continental slope (47°02.4'N and 139°57'E, water depth 1,004 m), is represented by silty clay sediment in the upper and lower parts and by clayey silt sediment in the middle part (**Figure 2**). There are three thinly laminated DLs in its middle part (**Figure 2**). The sediment lithology, productivity (total organic, chlorin and carbonate contents), stable oxygen ratio of planktic foraminifera and pollen records for the northern and central Sea of Japan (cores LV32-33 and LV53-23-1, respectively) with constructed age models were previously presented in (Gorbarenko et al., 2014; Gorbarenko et al., 2015). Several planktic foraminifera samples from the sediments of core LV32-33 and from core LV53-23-1 were dated by AMS ^{14}C (Gorbarenko et al., 2014; Gorbarenko et al., 2015, respectively).

Color Parameters

The color parameters L* and b* in the sediment cores LV53-23-1 and LV76-3-1 were measured aboard ship after core splitting at 1 cm intervals, using a spectrophotometer Minolta CM-700d. The parameter L* (psychometric lightness) showed variability in its white and black sediment coloring and decreased when the content of organic matter increased in the sediment; therefore this proxy is traditionally used to correlate dark and light layers in Sea of Japan sediments (Watanabe et al., 2007; Khim et al., 2009). The b* color parameter is mostly controlled by biogenic siliceous production and presents a useful tool for sediment correlation as well (Holbourn et al., 2002; Nürnberg and Tiedemann, 2004).

Besides the conventional color parameters, we measured the proportion of white to black color (photo lightness, PL) in sediment core LV76-3-1, using an original photo set (with a Canon 50D digital camera and EF 28 mm/F 2.8 lens), initially applied to core LV53-23-1 (Gorbarenko et al., 2015). The calculated PL values changed from zero (0) for the color black to 255 for white, with a resolution of 11 pixels per 1 mm. PL was measured aboard ship immediately after splitting the core into two halves and results were averaged with a resolution of 1 mm (Gorbarenko et al., 2015; Kolesnik et al., 2020). This gave a significantly higher resolution comparison than with a conventional measurement of the parameter L* by spectrophotometer.

Chlorin Content

As indicators of the darkness of sediments, total organic and carbonate contents were measured in the sediments of cores LV32-33 and LV53-23-1 (Gorbarenko et al., 2014; Gorbarenko

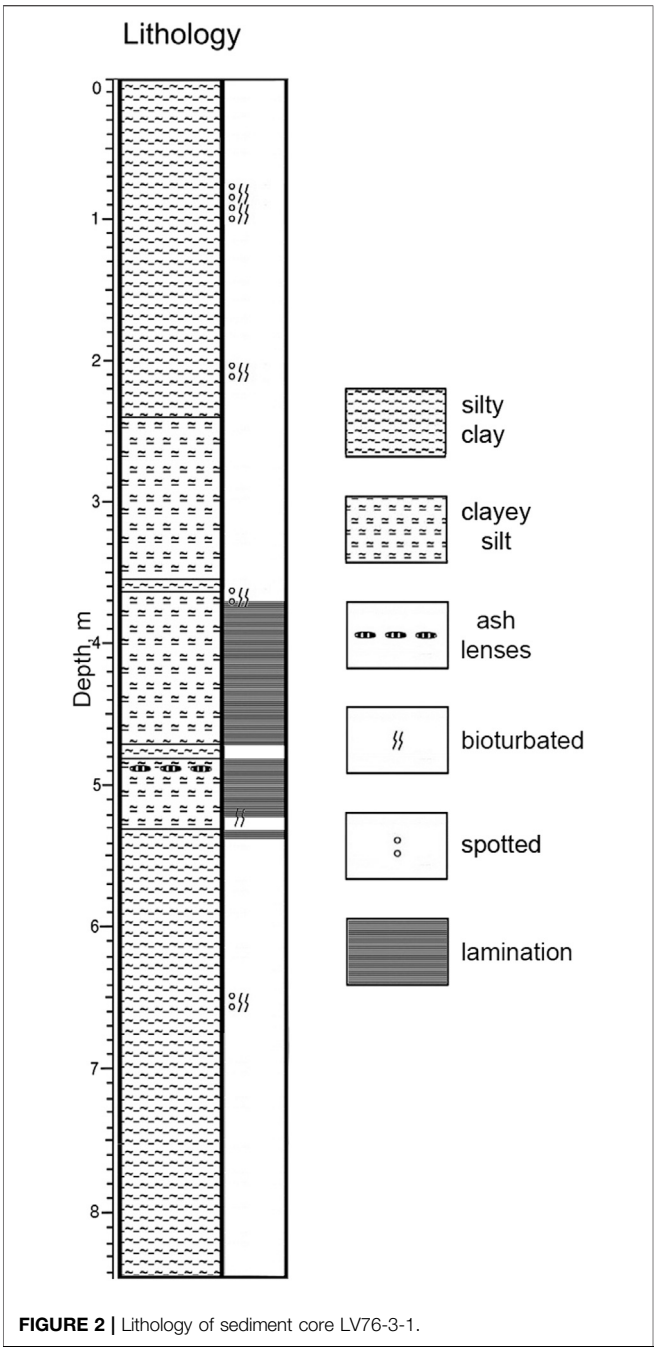

FIGURE 2 | Lithology of sediment core LV76-3-1.

et al., 2015). Here, we also used chlorin content to monitor the DLs, as it is a more sensitive indicator of the primary production and oxygenation of bottom sediments. Chlorin content was measured at 1 cm increments by using a Shimadzu UV-1650PC spectrophotometer, according to Harris et al. (1996) and with modification by Zakharkov et al. (2007). Chlorin, as a product of phytoplankton (chlorophyll a), is more easily destroyed in sediment compared with more resistant total organic carbon (TOC); as a result, it presents a more sensitive indicator of anoxic/euxinic conditions in the sediment and, therefore, DL formation (Gorbarenko et al., 2014; Gorbarenko et al., 2015) (**Figures 2**, **3**).

$\delta^{18}O$ of Planktic Foraminifera

Planktic foraminifera *Neogloboquadrina pachyderma* (s.), picked from the sediment fraction 125–250 μm, were analyzed for oxygen isotope composition ($\delta^{18}O$) by Finnigan-MAT 252 mass spectrometer, without preliminary oven roasting and with a modified sample preparation with relative standard deviations < 0.05‰ (Velivetskaya et al., 2009). The clean and white shells of the foraminifera *N. pachyderma* (s.) were picked under microscope with a step of 2 cm from the sediment intervals where its abundance was more than 40 individuals per sample; they were used for isotope analysis without additional cleaning.

Pollen Data

The pollen Kp index (the ratio of the warm species percentage to the total percentages of warm and cold species) and Kp* (the percentage of broadleaves and warm coniferous species in the pollen assemblages) were determined earlier in cores LV32-33 and LV53-23-1, respectively (Gorbarenko et al., 2014; Gorbarenko et al., 2015). These indexes indicate the total changes in the surrounding land vegetation and provide robust evidence of the regional climate variability suitable for correlation with records of the Northern Hemisphere climate changes, e.g., the $\delta^{18}O$ of the Greenland ice cores Seierstad et al., (2014) and the East Asian monsoon intensity (Wang et al., 2008).

Sediment Humidity

For humidity analysis, the sediment core LV76-3-1 was sampled into 10 cc cylinders, after core splitting at intervals of 5 cm, and weighed before and after drying at temperatures of 105°C up to a constant dry weight.

AMS ^{14}C Dating

Eleven planktic foraminifera samples were picked from the sediments of core LV32-33 and six samples from core LV53-23-1 were dated by AMS ^{14}C and published previously (Gorbarenko et al., 2014; Gorbarenko et al., 2015) (**Table 1**).

RESULTS

The color parameters (PL, L*, b*), humidity, chlorin content and $\delta^{18}O$ of planktic foraminifera *N. pachyderma* (s.) records of sediment core LV76-3-1 are shown in **Figure 3**. Three thinly laminated layers, outlined by the lithological description in **Figure 2**, were clearly confirmed as DLs by significant changes in the color parameters PL and L* and the higher chlorin content. The $\delta^{18}O$ of *N. pachyderma* (s.) value decreased in the middle laminated layer and dropped to less than 1 ‰ in the top of the upper laminated layer. This is consistent with the pattern of oxygen isotope changes in the Sea of Japan sediments over the laminated DLs 3 and 2, respectively (Oba et al., 1991; Yokoyama et al., 2007). Besides these three thinly laminated DLs, the color-induced PL, L* and b* and chlorin data indicated DL 1 above

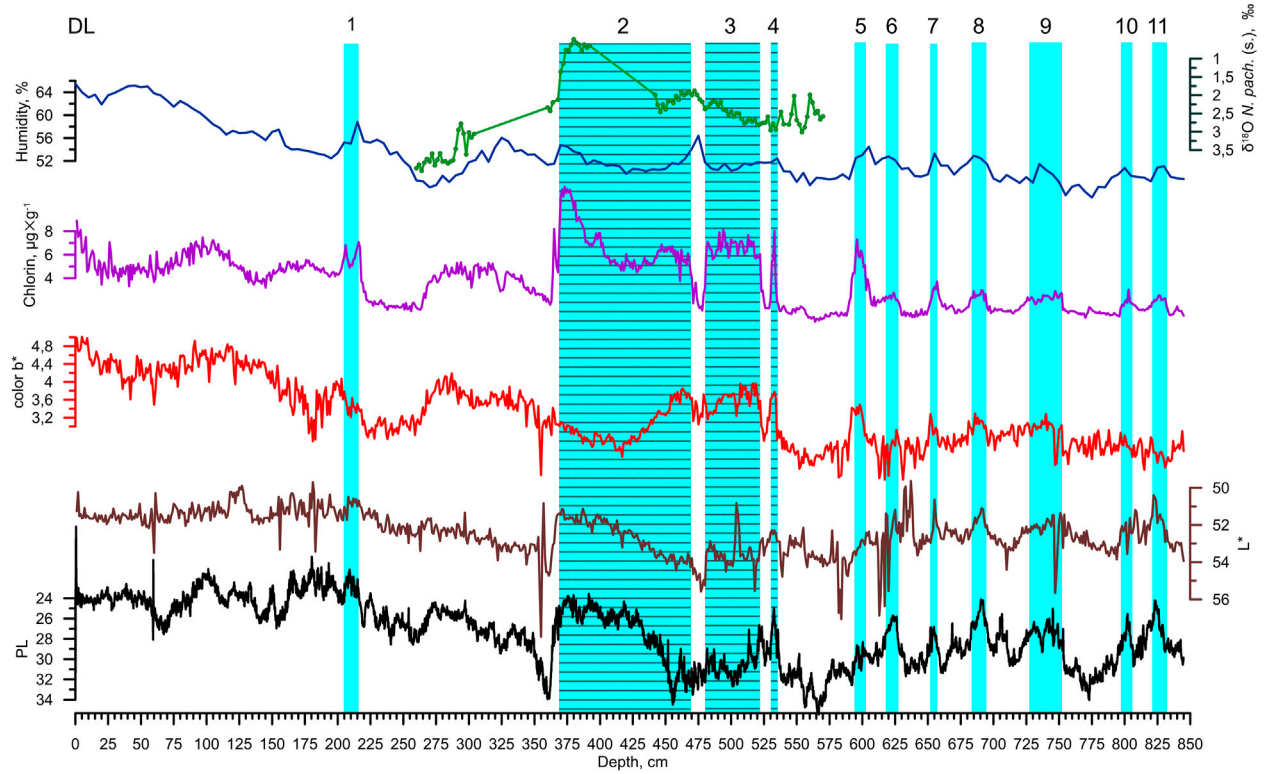

FIGURE 3 | Records of photo lightness (PL), color parameters L* and b*, humidity, chlorin content and $\delta^{18}O$ of planktic foraminifera *Neogloboquadrina pachyderma* (s.) in sediment core LV76-3-1 versus depth. Blue bars show the locations of the dark layers (DL). Hatched bars show thin laminated DLs. DL numbers are shown at the top.

TABLE 1 | AMS ^{14}C data on monospecies planktic foraminifera *N. pachyderma* (s.) for core LV53-23-1 (Gorbarenko et al., 2015) and LV32-33 (Gorbarenko et al., 2014). All measured ^{14}C age data were corrected for the Japan Sea surface water reservoir age of 400 years (Yokoyama et al., 2007). All radiocarbon ages were converted into calibrated 2-sigma calendar age ranges using the calibration program CALIB REV 7.0.1 (Stuiver and Reimer, 1993), with the Marine13 calibration curve (Reimer et al., 2013).

Accession #	Depth, cm	Foraminifera species	AMS ^{14}C age, yrs	Error, ± yr	Cal. age, ka
		LV53-23-1			
108922	40	*N. pachyderma* (s.) + *G.bulloides*	12,000	50	13.56
OS-103175	60	*N. pachyderma* (s.) + *G.bulloides*	15,200	45	18.07
112776					
108924	80	*N. pachyderma* (s.)	19,100	85	22.62
108925	110	*N. pachyderma* (s.)	23,500	140	27.39
108926	158	*N. pachyderma* (s.) + *G.bulloides*	29,300	270	32.92
OS-102784	208	*N. pachyderma* (s.) + *G.bulloides*	34,200	200	38.11
112777					
		LV32-33			
KIA 34207	105	*N. pachyderma* (s.)	5,235	40	5.63
KIA 34208	202.5	*N. pachyderma* (s.)	16,850	100	19.90
KIA 34209	212.5	*N. pachyderma* (s.)	17,520	110	20.73
KIA 34210	226.5	*N. pachyderma* (s.)	18,250	120	21.66
KIA 34211	300.5	*N. pachyderma* (s.)	20,660	150	24.51
KIA 34212	380	*N. pachyderma* (s.)	23,590	170	27.47
KIA 34213	412	*N. pachyderma* (s.)	24,530	240	28.28
KIA 34214	500	*N. pachyderma* (s.)	27,440	330	31.10
OS-102816	222-1	*N. pachyderma* (s.)	18,000	80	21.33
OS-102817	222-2	*N. pachyderma* (s.)	17,850	70	21.17
OS-102671	232-2	*N. pachyderma* (s.)	18,350	65	21.79

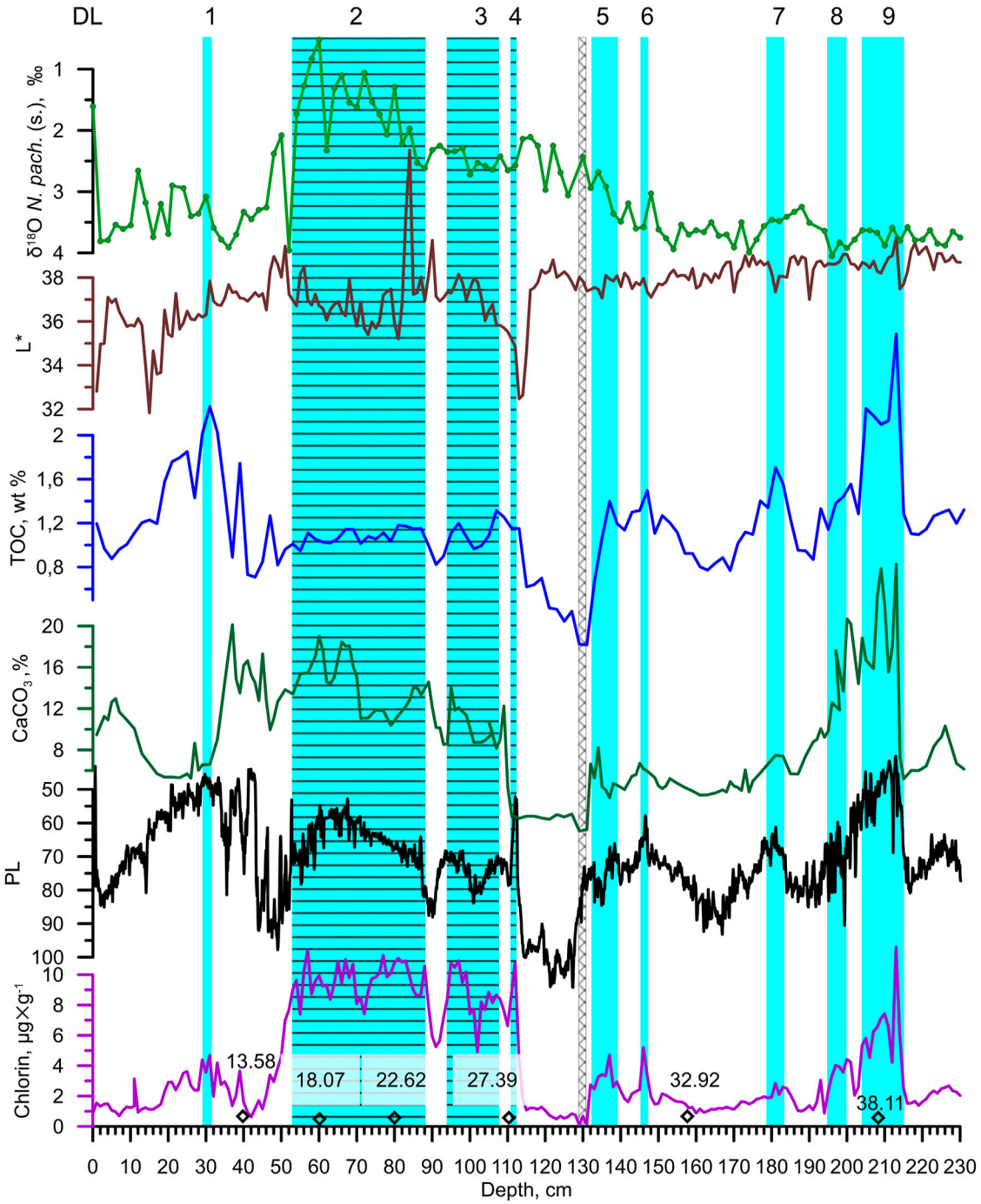

FIGURE 4 | Records of chlorin, total organic and carbonate content, number of planktic foraminifera per 1 g of dry sediments and $\delta^{18}O$ of planktic foraminifera *N. pachyderma* (s.) in sediment core LV53-23-1 versus depth. Diamonds indicate AMS 14C data (cal. ka). Notation of bars and DL number is the same as in **Figure 3**.

them and seven DLs (5–11) below throughout the core length (**Figure 3**).

The full sequence of DL formation in the central core LV53-23-1 over the interval 0–230 cm was outlined by productivity parameters (chlorin, TOC, $CaCO_3$ content), color proxies (PL and L*) and the $\delta^{18}O$ of *N. pachyderma* (s.) record presented earlier by Gorbarenko et al. (2015) (**Figure 4**). The pattern changes of $\delta^{18}O$ in planktic foraminifera outlined well the formation of DLs 3 and 2, similar to core LV76-3-1. The ash layer AT, with an age of nearly 30 ka (Smith et al., 2013), is located just above DL 5. Six AMS ^{14}C data confirmed well the age formation of DLs 1–9 (**Figure 4**).

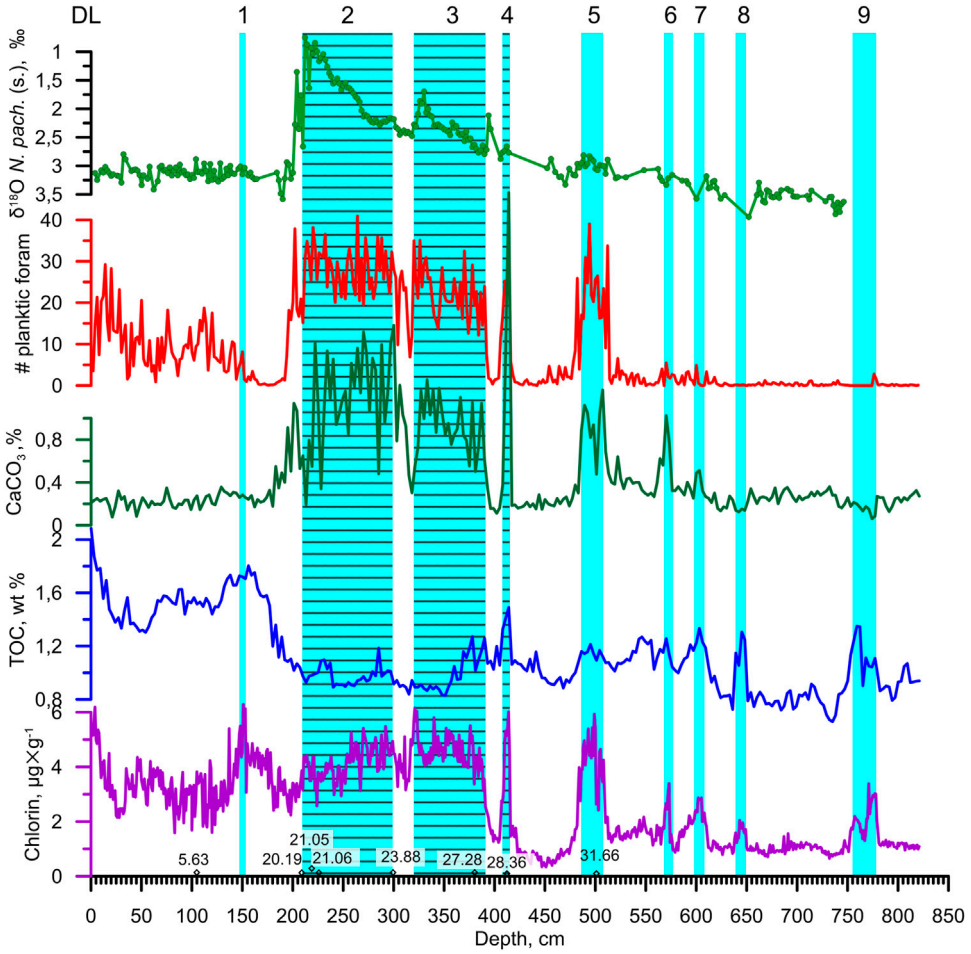

FIGURE 5 | Records of chlorin, total organic and carbonate content and photo lightness (PL), color parameter L* and $\delta^{18}O$ of planktic foraminifera *N. pachyderma* (s.) in sediment core LV32-33 versus depth. Notation of bars and DL number is the same as in **Figure 3**.

The sequence of DLs 1–9 in the north-western core LV32-33 was constructed by productivity proxies (TOC, $CaCO_3$ and chlorin contents), the abundance of planktic foraminifera in sediments, the $\delta^{18}O$ of *N. pachyderma* (s.) record and AMS ^{14}C data based on the published results (Gorbarenko et al., 2014) (**Figure 5**). However, the formation of DLs 2 and three in the sediments of this core were not accompanied by the enhanced content of TOC, contrary to its rising in other DLs.

DISCUSSION

In order to clarify the timing and mechanisms of DL formation in the Sea of Japan, sequences of DLs determined in the cores LV76-3-1, LV53-23-1 and LV32-33 (**Figures 3–5**) were correlated with the well-dated Greenland Interglacials (GIs) and Heinrich Stadials (HSs) of the following: the NGRIP $\delta^{18}O$ record (Seierstad et al., 2014), the summer East Asian monsoon intensity Wang et al. (2008) and the relative sea level (RSL) changes (Lambeck et al., 2014) (**Figure 6**, **Table 2**). In addition to the mentioned proxies of the studied cores, we presented here the pollen indices Kp and Kp* for cores LV32-33 and LV53-23-1, respectively, which were earlier presented in Gorbarenko et al. (2014) and Gorbarenko et al. (2015); they allowed us to correlate the formation of DLs with global climate changes in the Northern Hemisphere recorded in the $\delta^{18}O$ curves of the Greenland ice and East Asian monsoon.

The formation of DL 5, located just below the AT ash layer with an age of 30.0 ka, was most likely forced by the rapid fall of global sea level (by up to 40 m) after 30.7 ka Lambeck et al. (2014), Yokoyama et al. (2018), resulting in the decreased inflow of the saline water of the Tsushima Current into the Sea of Japan and the beginning of surface water freshening and, therefore, decreasing deep water ventilation and surface sediment oxygenation. According to the pollen indices Kp and Kp*, the climate conditions during this period were cold and, therefore, DL 5 may be correlated with cold HS 3. This is consistent with the AMS ^{14}C data in core LV32-33 from 31.1 ka (**Figure 6**). The formation of DL 4 was accompanied by an improvement in the regional climate conditions (a rise in Kp in the detailed core study of LV32-33), which may be related to GIs 4 or 3. The intensification of the summer East Asian monsoon resulted in an increase in surface water stratification and the growth of primary

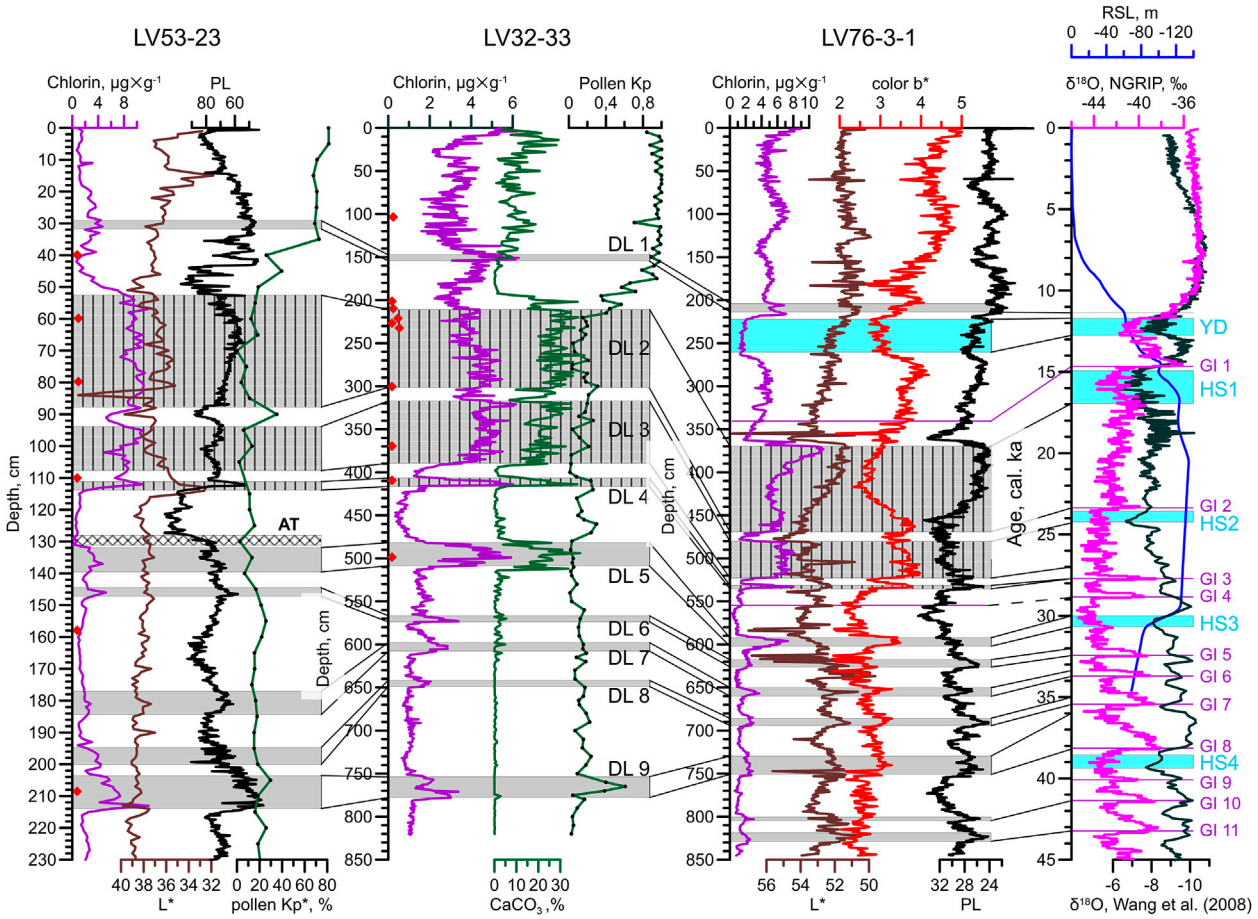

FIGURE 6 | Correlation of the photo lightness (PL), color parameters L* and b*, $CaCO_3$ and chlorin content and pollen-derived climate-induced Kp and Kp* indices in the cores LV53-23, LV32-33 and LV76-3-1 with Greenland Interglacials (GIs) and Heinrich Stadials (HSs) of NGRIP $\delta^{18}O$ record (Seierstad et al., 2014), summer East Asian monsoon intensity (Wang et al., 2008) and relative sea level (RSL) changes (Lambeck et al., 2014). Gray bars show the locations of the dark layers (DL). Hatched bars show thin laminated DLs. Blue bars show HSs 1–4 and cold Younger Dryas event (YD). Cross-hatched bar shows the location of tephra layer AT in core LV53-23. Purple horizontal lines indicate GIs. Red rhombs indicate AMS ^{14}C dating of cores LV32-33 and LV53-23-1.

productivity in the Sea of Japan. We suggested that the formation of the laminated DL 4 was correlated with GI 3 because of a coeval decrease in $\delta^{18}O$ stalagmites from the Chinese caves and long sediment intervals between the upper boundary of DL 5 and the laminated DL 4 in all three cores, which required a long time for sedimentation (**Figure 6**). Detailed curves of the PL and L* color proxies, presented in core LV76-3-1, allowed us to suggest that GI 4 also influenced the Sea of Japan's environment and sedimentation and was recorded in this core at a length of 555 cm, without forming a pronounced DL (**Figure 6**).

According to our correlation, a laminated DL 3 commenced at nearly 27 ka and continued up to the onset of the cold HS 2. Detailed pollen records from core LV32-33 allowed us to suggest that the light layer between the laminated DLs 3 and 2 was associated with regional climate cooling, decreasing summer East Asian monsoon intensity, surface water stratification and a productivity coeval with cold HS 2.

Laminated DLs 3 and 2 were associated with the lowest global sea levels and significant shrinkage of the input of the saline Tsushima Current into the Sea of Japan through the shallow Tsushima Strait during the LGM (**Figure 6**). Under the prevailing precipitation above evaporation in the Sea of Japan region, a decrease of Tsushima Current inflow led to a decrease in the surface-water salinity, strengthening its stratification and, therefore, led to a dramatic decrease in deep water ventilation. As a result, a cessation of deep water ventilation led to oxygen deficit conditions in the surface sediments and to the formation of the DLs, which is consistent with earlier conclusions (Gorbarenko, 1983; Gorbarenko, 1993; Oba et al., 1991; Matsui et al., 1998; Tada et al., 1999). According to our correlations, the formation of laminated DL 2 occurred after GI 2, coeval with summer East Asian monsoon intensification and an age of 23.5 ka. This continued up to the start of HS 1 (17.0 ka), synchronous with a rise in global sea level (**Figure 6**). The inferred ages of the laminated DLs 3 and 2 are consistent with available AMS data and close to the reconstruction by Yokoyama et al. (2007), based on the investigation of the dated MD01-2407 and DGC-6 cores, and to the estimation by Ishihama et al. (2014), based on

TABLE 2 | Ages of dark layer sequence in the Japan Sea over the last 40 kyr and mechanisms of its formation.

Dark layer No	Mechanism origin	Age, cal. ka
1	EASM intensification	11.4
2	LGM sea level low stand	17.0–23.5
3	LGM sea level low stand	24.2–27.0
4	GI3	27.8
5	Rapid RSL fall, HS3	30.0–30.7
6	GI5	32.0–32.5
7	GI6	33.4–33.8
8	GI7	35.0–35.5
9	GI8	37.0–38.2

*Note: **Table 2** would be better titled as "Key time points of the abrupt changes in the Japan Sea surface water parameters like density and productivity". Actually, the surface water conditions are primary drivers of water ventilation in the Japan Sea and deep water oxygenation that led to dark layer's formation at the bottom at the oxygen deficit periods. Here we prefer to follow customary practice in the Japan Sea investigation.*

sediment core MD179-3312 from the far south-eastern part of the sea (off Joetsu) (**Figure 1**).

The high sedimentation rate in core LV76-3-1 during the late deglaciation and Holocene allowed us to detect the effect of a Bølling-Ållerød warming and Younger Dryas (YD) cooling on the Sea of Japan, as well as sedimentation, by using the related responses of productivity and color proxies (**Figure 6**). The generalized pollen parameters, Kp and Kp*, show a trend of regional climate warming during these periods; however, the species distribution in pollen assemblages indicates a more complicated pattern of climate changes associated with Bølling-Ållerød warming and subsequent YD cooling (Gorbarenko et al., 2014, Gorbarenko et al., 2015). The formation of the laminated DL 1, with an age of 11.4 ka Yokoyama et al. (2007), was most likely forced by the enhancement of the summer East Asian monsoon at the beginning of the Holocene, increasing productivity in the Sea of Japan and organic fluxes into the bottom, which significantly consume oxygen in the surface sediments (**Figure 6**).

The sequence of the DLs 9, 8, seven and 6 in the sediments of the Sea of Japan was associated with GIs 8, 7, 6 and 5, respectively, and the relative East Asian monsoon intensifications during Chinese interstadials (**Figure 6**). This is consistent with the hypotheses of Tada et al. (1999) under moderate sea level standing. The long-lasting GI 8 was accompanied by significant regional climate warming in the Sea of Japan according to pollen records, a rise in productivity and the intensive formation of DL 9. It seems probable that DLs 10 and 11, recorded in the northern core LV76-3-1, were associated with GIs 10 and 11, respectively (**Figure 6**). GI 9 was weakly detected in the sediment of the studied cores (**Figure 6**). With respect to the results of the multiproxy correlation of the three cores, the ages and origin of the DLs in the Sea of Japan over the last 40 kyr are shown in **Table 1**.

Need to note, that not all of the DLs 1–9 established by us over the last 40 kyr can be found in sediments of the whole Sea of Japan. Depositional mechanisms responsible for individual DL formation vary throughout the area and sea depth depending on sediment oxygenation, organic matter fluxes and the rate of sedimentation, resulting in wide ranges of DL sediment fabrics (Watanabe et al., 2007). Here we mostly outlined the sequence in the variability of the surface water conditions over the last 40 kyr determined by different mechanisms (millennial scale climate and global sea level changes) that mainly governed the DL formation in the Sea of Japan.

CONCLUSION

The unique geographical location of the marginal Sea of Japan and its constrained water exchange with the western Pacific through shallow straits determined very specific responses in its environment and sedimentation and millennial scale climate change with the formation of decimeter to centimeter alternations of dark and light layers. Meanwhile, the ages and mechanisms responsible for their formation during the last 40°kyr, accompanied by dramatic changes in climate, the continental ice sheets dynamic and sea level changes, had not been fully determined.

Original, highly resolved color PL, the conventional color parameters L* and b*, AMS ^{14}C data, chlorin and $CaCO_3$ content and pollen climate parameters allowed the correlation of the DLs in three cores from the northern and central parts of the Sea of Japan with well-dated GIs, HSs, the summer East Asian monsoon intensity and sea level changes.

DLs 9, 8, 7 and 6, formed after HS 4, were triggered by Greenland interstadials 8, 7, 6 and 5, respectively. It is consistent with the conclusion of Tada et al. (1999) that they were coeval with the intensification of the summer East Asian monsoon and increasing surface water stratification and productivity. The long-lasting GI 8 was accompanied by significant climate warming, which led to the formation of a more intense DL. The accumulation of DL 5 was forced by a rapid global sea level fall, coeval with HS 3, as a result of the decreasing saline Tsushima Current water input through the shallow Tsushima Strait and the increasing surface water stratification and falling deep water ventilation. DL four was probably launched by GI 3, as well as the intensification of the summer East Asian monsoon. Further global sea level falling during the LGM led to the formation of laminated DLs 3 and 2 during the periods 27.0–24.2 ka and 23.5–17.0 ka, respectively. The interruption of the formation of these DLs was likely related to more severe environmental conditions in the Sea of Japan during HS 2 and weak productivity. DL 1 was associated with significant summer East Asian monsoon intensification and environmental warming, following the YD cold event at the onset of the Holocene and a significant increase in productivity.

The established timing of the formation of DLs 1–5 in the Japan Sea sediments initially outlined the abrupt changes in surface water conditions such as density and productivity, which further forced changes in deep water ventilation, resulting in the formation of dark/light layers.

DATA AVAILABILITY STATEMENT

The raw data supporting the conclusion of this article will be made available by the authors, without undue reservation.

AUTHOR CONTRIBUTIONS

SG wrote the manuscript, designed its structure, and analyzed the data collected. XS critically revised the manuscript. AB, YL, AA, JZ, EY, YV, YW, and LH helped in collecting and analyzing the data.

FUNDING

This work was supported by the Russian Foundation for Basic Research (19–05–00663a), Russian state budget theme No. 7 AAAA-A17-1170301100330 of POI FEB RAS, the National Natural Science Foundation of China (41876065, 41476056, 41611130042 and U1606401), the National Program on Global Change and Air-Sea Interaction (Grant Nos. GASI-GEOGE-04), the International Cooperative Project in Polar Regions (201613), the Russian Scientific Fund # 19-77-10030 and the National Program on Global Change and Air-Sea Interaction (Grant No. GASI-GEOGE-03).

ACKNOWLEDGMENTS

We are grateful to Professor Tadamichi Oba and Professor Ryuji Tada for their fruitful cooperation.

REFERENCES

Behl, R. J., and Kennett, J. P. (1996). Brief Interstadial Events in the Santa Barbara basin, NE Pacific, during the Past 60 Kyr. *Nature* 379, 243–246. doi:10.1038/379243a0

Gallagher, S. J., Kitamura, A., Iryu, Y., Itaki, T., Koizumi, I., and Hoiles, P. W. (2015). The Pliocene to Recent History of the Kuroshio and Tsushima Currents: a Multi-Proxy Approach. *Prog. Earth Planet. Sci.* 2, 17. doi:10.1186/s40645-015-0045-6

Gamo, T., Nakayama, N., Takahata, N., Sano, Y., Zhang, J., Yamazaki, E., et al. (2014). The Sea of Japan and its Unique Chemistry Revealed by Time-Series Observations over the Last 30 Years. *Monogr. Environ. Earth Planets* 2, 1–22. doi:10.5047/meep.2014.00201.0001

Gorbarenko, S. A., Malakhova, G. Y., Artemova, A. V., Bosin, A. A., Yanchenko, E. A., and Vasilenko, Y. (2019). Millennial Scale Cycles in the Bering Sea during Penultimate and Last Glacials; Their Similarities and Differences. *Quat. Int.* 525, 151–158. doi:10.1016/j.quaint.2019.07.016

Gorbarenko, S. A., Nam, S.-I., Rybiakova, Y. V., Shi, X., Liu, Y., and Bosin, A. A. (2014). High Resolution Climate and Environmental Changes of the Northern Japan (East) Sea for the Last 40kyr Inferred from Sedimentary Geochemical and Pollen Data. *Palaeogeogr. Palaeoclimatol. Palaeoecol.* 414, 260–272. doi:10.1016/j.palaeo.2014.09.001

Gorbarenko, S. A. (1983). Paleogeographic Conditions in the central Part of the Sea of Japan during Holocene and Late Pleistocene from the Data on 18O/16O in Foraminiferal Tests (In Russian with English Abstract). *Oceanology* 23, 300–303.

Gorbarenko, S. A. (1993). The Reasons for Freshening of Surface Water Mass in Sea of Japan during the Latest Glaciation Determined from Ratios of Oxygen Isotopes in Planktonic Foraminifera. *Oceanology* 33, 359–364.

Gorbarenko, S., Shi, X., Rybiakova, Y., Bosin, A., Malakhov, M., Zou, J., et al. (2015). Fine Structure of Dark Layers in the central Japan Sea and Their Relationship with the Abrupt Climate and Sea Level Changes over the Last 75ka Inferred from Lithophysical, Geochemical and Pollen Results. *J. Asian Earth Sci.* 114, 476–487. doi:10.1016/j.jseaes.2015.04.040

Harris, P. G., Zhao, M., Rosell-Melé, A., Tiedemann, R., Sarnthein, M., and Maxwell, J. R. (1996). Chlorin Accumulation Rate as a Proxy for Quaternary marine Primary Productivity. *Nature* 383, 63–65. doi:10.1038/383063a0

Holbourn, A. E., Kiefer, T., Pflaumann, U., and Rothe, S. (2002). *WEPAMA Cruise MD 122/IMAGES VII*. Rapp, France: Plouzane.

Ishihama, S., Oi, T., Hasegawa, S., and Matsumoto, R. (2014). Paleoceanographic Changes of Surface and Deep Water Based on Oxygen and Carbon Isotope Records during the Last 130kyr Identified in MD179 Cores, off Joetsu, Japan Sea. *J. Asian Earth Sci.* 90, 254–265. doi:10.1016/j.jseaes.2013.12.020

Keigwin, L. D., and Gorbarenko, S. A. (1992). Sea Level, Surface Salinity of the Japan Sea, and the Younger Dryas Event in the Northwestern Pacific Ocean. *Quat. Res.* 37, 346–360. doi:10.1016/0033-5894(92)90072-Q

Khim, B.-K., Tada, R., Park, Y. H., Bahk, J. J., Kido, Y., Itaki, T., et al. (2009). Correlation of TL Layers for the Synchronous Paleoceanographic Events in the East Sea (Sea of Japan) during the Late Quaternary. *Geosci. J.* 13, 113–120. doi:10.1007/s12303-009-0010-8

Kido, Y., Minami, I., Tada, R., Fujine, K., Irino, T., Ikehara, K., et al. (2007). Orbital-scale Stratigraphy and High-Resolution Analysis of Biogenic Components and Deep-Water Oxygenation Conditions in the Japan Sea during the Last 640 Kyr. *Palaeogeogr. Palaeoclimatol. Palaeoecol.* 247, 32–49. doi:10.1016/j.palaeo.2006.11.020

Kim, K.-R., Kim, G., Kim, K., Lobanov, V., Ponomarev, V., and Salyuk, A. (2002). A Sudden Bottom-Water Formation during the Severe winter 2000-2001: The Case of the East/Japan Sea. *Geophys. Res. Lett.* 29, 75–175–4. doi:10.1029/2001GL014498

Kolesnik, A. N., Bosin, A. A., Kolesnik, O. N., Yanchenko, E. A., and Vasilenko, Y. P. (2020). New Method to Obtain Quantified Data on Color of Marine Sediments. *Dokl. Earth Sc.* 495, 845–849. doi:10.1134/S1028334X20110070

Lambeck, K., Rouby, H., Purcell, A., Sun, Y., and Sambridge, M. (2014). Sea Level and Global Ice Volumes from the Last Glacial Maximum to the Holocene. *Proc. Natl. Acad. Sci.* 111, 15296–15303. doi:10.1073/pnas.1411762111

Matsui, H., Tada, R., and Oba, T. (1998). Low-Salinity Isolation Event in the Japan Sea in Response to Eustatic Sea-Level Drop during LGM: Reconstruction Based on Salinity-Balance Model. *Daiyonki-kenkyu* 37, 221–233. doi:10.4116/jaqua.37.221

Nagashima, K., Tada, R., Matsui, H., Irino, T., Tani, A., and Toyoda, S. (2007). Orbital- and Millennial-Scale Variations in Asian Dust Transport Path to the Japan Sea. *Palaeogeogr. Palaeoclimatol. Palaeoecol.* 247, 144–161. doi:10.1016/j.palaeo.2006.11.027

Nagashima, K., Tada, R., Tani, A., Sun, Y., Isozaki, Y., Toyoda, S., et al. (2011). Millennial-scale Oscillations of the westerly Jet Path during the Last Glacial Period. *J. Asian Earth Sci.* 40, 1214–1220. doi:10.1016/j.jseaes.2010.08.010

Nürnberg, D., and Tiedemann, R. (2004). Environmental Change in the Sea of Okhotsk during the Last 1.1 Million Years. *Paleoceanography* 19, a–n. doi:10.1029/2004pa001023

Oba, T., Kato, M., Kitazato, H., Koizumi, I., Omura, A., Sakai, T., et al. (1991). Paleoenvironmental Changes in the Japan Sea during the Last 85,000 Years. *Paleoceanography* 6, 499–518. doi:10.1029/91PA00560

Oba, T. (1984). The Japan Sea since the Last Glacial Age; Paleoenvironmetal History - Mainly Based on Analysis of Core KH-79-3, C-3 (In Japanese). *Chikyu* 6, 571–575.

Riethdorf, J.-R., Nürnberg, D., Max, L., Tiedemann, R., Gorbarenko, S. A., and Malakhov, M. I. (2013). Millennial-scale Variability of marine Productivity and Terrigenous Matter Supply in the Western Bering Sea over the Past 180 Kyr. *Clim. Past* 9, 1345–1373. doi:10.5194/cp-9-1345-2013

Seierstad, I. K., Abbott, P. M., Bigler, M., Blunier, T., Bourne, A. J., Brook, E., et al. (2014). Consistently Dated Records from the Greenland GRIP, GISP2 and NGRIP Ice Cores for the Past 104 Ka Reveal Regional Millennial-Scale δ18O Gradients with Possible Heinrich Event Imprint. *Quat. Sci. Rev.* 106, 29–46. doi:10.1016/j.quascirev.2014.10.032

Smith, V. C., Staff, R. A., Blockley, S. P. E., Bronk Ramsey, C., Nakagawa, T., Mark, D. F., et al. (2013). Identification and Correlation of Visible Tephras in the Lake Suigetsu SG06 Sedimentary Archive, Japan: Chronostratigraphic Markers for Synchronising of East Asian/west Pacific Palaeoclimatic Records across the Last 150 Ka. *Quat. Sci. Rev.* 67, 121–137. doi:10.1016/j.quascirev.2013.01.026

Tada, R., Irino, T., Ikehara, K., Karasuda, A., Sugisaki, S., Xuan, C., et al. (2018). High-resolution and High-Precision Correlation of Dark and Light Layers in the Quaternary Hemipelagic Sediments of the Japan Sea Recovered during IODP Expedition 346. *Prog. Earth Planet. Sci.* 5, 19. doi:10.1186/s40645-018-0167-8

Tada, R., Irino, T., and Koizumi, I. (1999). Land-ocean Linkages over Orbital and Millennial Timescales Recorded in Late Quaternary Sediments of the Japan Sea. *Paleoceanography* 14, 236–247. doi:10.1029/1998PA900016

Tada, R., Irino, T., and Koizumi, I. (1995). "Possible Dansgaard–Oeschger Oscillation Signal Recorded in the Japan Sea Sediments," in *Global Fluxes of Carbon and its Related Substances in the Coastal Sea–Ocean Atmospheric System*. Editors S. Tsunogai, L. Iseki, I. Koike, and T. Oba (Minato, Japan: Yokohama, M&J International)), 517–522.

Tada, R., Koizumi, I., Cramp, A., and Rahman, A. (1992). "Correlation of Dark and Light Layers, and the Origin of Their Cyclicity in the Quaternary Sediments from the Japan Sea," in *Proceedings of the Ocean Drilling Program, 127/128 Part 1 Scientific Results* (National Science Foundation, Texas Joint Oceanographic Institutions, Inc., Texas), 577–601. doi:10.2973/odp.proc.sr.127128-1.160.1992

Talley, L., Min, D.-H., Lobanov, V., Luchin, V., Ponomarev, V., Salyuk, A., et al. (2006). Japan/East Sea Water Masses and Their Relation to the Sea's Circulation. *Oceanog.* 19, 32–49. doi:10.5670/oceanog.2006.42

Velivetskaya, T. A., Ignatiev, A. V., and Gorbarenko, S. A. (2009). Carbon and Oxygen Isotope Microanalysis of Carbonate. *Rapid Commun. Mass. Spectrom.* 23, 2391–2397. doi:10.1002/rcm.3989

Wang, Y., Cheng, H., Edwards, R. L., Kong, X., Shao, X., Chen, S., et al. (2008). Millennial- and Orbital-Scale Changes in the East Asian Monsoon over the Past 224,000 Years. *Nature* 451, 1090–1093. doi:10.1038/nature06692

Watanabe, S., Tada, R., Ikehara, K., Fujine, K., and Kido, Y. (2007). Sediment Fabrics, Oxygenation History, and Circulation Modes of Japan Sea during the Late Quaternary. *Palaeogeogr. Palaeoclimatol. Palaeoecol.* 247, 50–64. doi:10.1016/j.palaeo.2006.11.021

Yokoyama, Y., Esat, T. M., Thompson, W. G., Thomas, A. L., Webster, J. M., Miyairi, Y., et al. (2018). Rapid Glaciation and a Two-step Sea Level Plunge into the Last Glacial Maximum. *Nature* 559, 603–607. doi:10.1038/s41586-018-0335-4

Yokoyama, Y., Kido, Y., Tada, R., Minami, I., Finkel, R. C., and Matsuzaki, H. (2007). Japan Sea Oxygen Isotope Stratigraphy and Global Sea-Level Changes for the Last 50,000 Years Recorded in Sediment Cores from the Oki Ridge. *Palaeogeogr. Palaeoclimatol. Palaeoecol.* 247, 5–17. doi:10.1016/j.palaeo.2006.11.018

Zakharkov, S. P., Gorbarenko, S. A., and Bosin, A. A. (2007). Chlorin Content in Sea Sediments as an Indication of Sea Primary Productivity (In Russian). *Bull. Far East. Branch Russ. Acad. Sci.* 1, 52–58.

Conflict of Interest: The authors declare that the research was conducted in the absence of any commercial or financial relationships that could be construed as a potential conflict of interest.

Copyright © 2021 Gorbarenko, Shi, Bosin, Liu, Artemova, Zou, Yanchenko, Vasilenko, Wu and Hu. This is an open-access article distributed under the terms of the Creative Commons Attribution License (CC BY). The use, distribution or reproduction in other forums is permitted, provided the original author(s) and the copyright owner(s) are credited and that the original publication in this journal is cited, in accordance with accepted academic practice. No use, distribution or reproduction is permitted which does not comply with these terms.